horticulturae

MDPI

Article

Differences in Saprophytic Growth, Virulence, Genomes, and Secretomes of *Ilyonectria robusta* and *I. mors-panacis* Isolates from Roots of American Ginseng (*Panax quinquefolius*)

Behrang Behdarvandi, Tom Hsiang, Moez Valliani and Paul H. Goodwin *

School of Environmental Sciences, University of Guelph, 50 Stone Road East, Guelph, ON N1G 2W1, Canada; bbehdarv@uoguelph.ca (B.B.); thsiang@uoguelph.ca (T.H.); mvallian@uoguelph.ca (M.V.)
* Correspondence: pgoodwin@uoguelph.ca

Abstract: A comparison of the virulence, saprophytic growth, and genomes of 12 isolates of *Ilyonectria mors-panacis* and 4 isolates of *I. robusta* from Canada pathogenic to *Panax quinquefolius* was made. There were no significant differences in the average lesion size on detached roots between isolates of the two *Ilyonectria* species or isolates that originated from infected roots in first- or second-crop ginseng soils. This did not support the hypotheses that *I. mors-panacis* is always more virulent than *I. robusta* or that there is selection for higher virulence during the first crop. However, the average growth rate on potato dextrose agar for *I. robusta* was significantly greater than that of *I. mors-panacis*, and the average total genome size of *I. robusta* isolates was significantly smaller with a significantly higher GC content. On dendrograms based on nucleotide sequences of all predicted exons of the genomes, *I. robusta* isolates were distinguishable from *I. mors-panacis* isolates, which were similar but could be separated into types 1 and 2. The difference between type 1 and type 2 *I. mors-panacis* was not related to geographical origin, virulence, growth rate, or mating type. However, the division was also observed for the total predicted secretome, most notably small secreted cysteine-rich proteins and secreted proteases, indicating that type 1 and 2 isolates of *I. mors-panacis* may interact differently with their environment.

Keywords: *Ilyonectria robusta*; *Ilyonectria mors-panacis*; *Ilyonectria* genomes; *Panax quinquefolius* genomic analysis; secretome proteins; non-secretome proteins

Citation: Behdarvandi, B.; Hsiang, T.; Valliani, M.; Goodwin, P.H. Differences in Saprophytic Growth, Virulence, Genomes, and Secretomes of *Ilyonectria robusta* and *I. mors-panacis* Isolates from Roots of American Ginseng (*Panax quinquefolius*). *Horticulturae* **2023**, *9*, 713. https://doi.org/10.3390/horticulturae9060713

Received: 27 May 2023
Revised: 8 June 2023
Accepted: 13 June 2023
Published: 17 June 2023

1. Introduction

Ilyonectria spp. are soil-borne fungi that can cause root rot in apples [1], grapevines [2], ginseng [3], and other plants [4]. In ginseng, *Ilyonectria* spp. produce red to dark brown lesions on roots, wilting, reddish aerial parts, and plant death [5,6]. Cabral et al. [4] proposed 18 species of *Ilyonectria* spp. in the *Ilyonectria radicicola* complex, which had previously been placed in the anamorphic genera *Cylindrocarpon* and *Ramularia* and the teleomorphic genus *Neonectria*. Among the species in the *I. radicicola* complex, *Ilyonectria mors-panacis*, *I. crassa*, *I. panacis*, and *I. robusta* were described as pathogens of ginseng roots.

Ilyonectria spp. from ginseng (previously known as *Cylindrocarpon destructans*) are reported to vary in virulence, morphology, and DNA sequences commonly used for taxonomic purposes. Based on the final stand count of ginseng seedlings in inoculated soil, Seifert et al. [3] divided *C. destructans* into highly and weakly virulent isolates, with the highly virulent ones forming a monophyletic group with identical ITS and β-tubulin sequences matching those of *C. destructans* f. sp. *panacis* [7], while the weakly virulent isolates were more diversely related to other *Cylindrocarpon* isolates from angiosperms and conifers. Cabral et al. [4] later reclassified *C. destructans* f. sp. *panacis* as *I. mors-panacis*. Song et al. [8] also divided isolates of *C. destructans* into weakly and highly virulent pathogenicity groups based on percent seedling emergence of *Panax ginseng* in infested soils and lesion size of wounded inoculated roots. Based on ITS and mt SSU rDNA sequences, they also showed

that highly virulent isolates were highly similar, while weakly virulent isolates were more diverse, clustering into several groups. Seo et al. [9] showed that highly virulent isolates from *P. ginseng* roots were mainly *I. mors-panacis*, while weakly virulent isolates were *I. liriodendra*, *I. cyclaminicola*, *I. robusta*, or *I. venezuelensis*.

Ilyonectria mors-panacis is the most common soil fungus associated with ginseng replant disease [10]. It can cause relatively low levels of root rot with localized black-brown lesions or severe root rot known as disappearing root rot, which is often found in second crop soil (i.e., soil where a previous crop of ginseng was grown), with almost complete breakdown of the root cortex leaving only the dead epidermis, which together is called replant disease [11–14]. One hypothesis is that replant disease is due to selection for highly virulent isolates that reproduce more in the first crop, resulting in more virulent isolates in the second crop soil [15]. Although many studies have reported differences in the virulence of *Ilyonectria* isolates from diseased ginseng roots, it is often not noted if they were isolated from diseased roots growing in replant or non-replant soil [8,9,12].

Most studies on variation among *Ilyonectria* isolates from ginseng have focused on a limited number of genes [3,4,8]. However, genetic variation among fungal plant pathogens can be compared using complete genomes instead of a few genes. Particular interest has been focused on studying the secretomes of fungal plant pathogens because secreted proteins can manipulate host cells during infection to obtain nutrients and suppress plant defenses [16]. The fungal secretome includes plant cell wall-degrading enzymes, small secreted proteins (SSPs), carbohydrate-active enzymes (CAZymes), lipases, and proteases [17,18]. For example, genomic comparisons [19] revealed that one third of the secreted proteins of 15 *Heterobasidion parviporum* isolates causing root and butt rot disease of Norway spruce, such as cytochrome P450 and acid protease, may contribute to virulence based on partial deletions in the genomes of the most weakly virulent isolate compared to the most highly virulent isolate. Analysis of secreted effectors in five subspecies of *Blumeria graminis*, which causes powdery mildew in grasses, showed that gene duplication and loss were responsible for the diversity of effectors contributing to host specificity [20].

There is a lack of information about the variation in virulence, growth rates, and genome sequences of isolates of *I. mors-panacis* and *I. robusta* from diseased ginseng roots. Thus far, reports on the genomic analysis of *Ilyonectria* spp. are limited. Guan et al. [21] sequenced the genome of *I. robusta* CD-56 isolated from *P. ginseng* with rusty root symptoms and predicted 498 genes in the secretome, with 7 genes for effectors and 129 genes for CAZymes. Zhu et al. [22] sequenced the genome of *I. mors-panacis* G3B isolated from *Panax notoginseng* with rusty root symptoms and found 120 genes potentially related to pathogenesis, including 7 genes for effectors and 28 genes for plant cell wall-degrading enzymes. The purpose of this study was to examine the growth rates, virulence, and predicted gene sets for proteins and secretomes of isolates mostly from infected roots of *Panax quinquefolius* grown in replant or non-replant gardens in Ontario and British Columbia, Canada. Assessment of their identity was done using the histone H3 sequence, virulence by inoculating detached roots with conidial suspensions, and growth rate in agar culture. Their sequenced and assembled genomes were used to identify genomic differences by comparing all predicted genes as well as elements of the secretome and the non-secretome.

2. Materials and Methods

2.1. Isolates

Isolates of *Ilyonectria* spp. were collected from diseased roots of American ginseng grown in replant or non-replant soil in Ontario or were received from the Summerland Research and Development Centre of Agriculture and Agri-Food Canada, BC, or the Canadian Collection of Fungal Cultures, Ottawa (CCFC). The *Ilyonectria* isolates collected from ginseng in Ontario were from surface-sterilized 2–3 year old symptomatic roots in gardens where roots were not treated with fungicides but the soil was fumigated with metam sodium or chloropicrin a year before planting. The isolates were maintained on

PDA (potato dextrose agar) in the dark at 22 °C for up to 4 weeks and also stored in 10% sterile glycerol (Fisher Scientific, Mississauga, ON, Canada) at −70 °C.

2.2. Histone H3 Sequencing

Isolates were cultured on sterilized cellophane sheets on PDA for a week. The mycelium (100 mg) was then harvested and DNA extracted following Edwards et al. [23], which, in brief, involves macerating the fungal tissue in buffer (200 mM Tris-HCl pH 7.5, 250 mM NaCl, 25 mM EDTA, 0.5% SDS), centrifuging, decanting, and precipitating with cold isopropanol, and resuspending the pellet in TE. The PCR for histone H3 sequencing consisted of 2.5 µL of 1X Tsg buffer, 1.87 µL of 1.5 mM $MgSO_4$, 0.08 µL of 32 µM dNTP, and 0.6 µL of 10 ng/mL of each H3 primer (F: AGGTCCACTGGTGGCAAG and R: AGCTGGATGTCCTTGGACTG [4], 0.2 µL (5 u/µL) *Tsg* polymerase (Bio Basic, Markham, ON, Canada), and 1 µL DNA (10-30 ng/µL) of each isolate in a final volume of 25 µL. Amplification conditions were 1 cycle at 94 °C for 5 min, followed by 40 cycles of 94 °C for 30 s, 52 °C for 30 s, and 72 °C for 80 s, with a final cycle of 72 °C for 10 min using an Eppendorf AG 22331 Thermocycler (Eppendorf, Hamburg, Germany). PCR without DNA was used as a control. PCR products were sequenced by the University of Guelph Laboratory Services, Guelph, ON, Canada. The sequences were examined using BLASTN against the nr/nt database through NCBI BLAST (blast.ncbi.nlm.nih.gov/Blast.cgi, accessed on 15 December 2017).

2.3. Isolate Growth Rate and Virulence

Isolates were cultured on PDA in the dark at 22 °C for 12 days. The growth rate was determined with eight replicates on three plates per replication by measuring the diameter (cm) of each culture. To test for virulence, isolates were cultured on V8 agar for 4 weeks in the dark, and then conidia were harvested and adjusted in dsH_2O to 1×10^6 spores/mL. *Panax quinquefolius* roots (3–4 year-old) were collected and stored at 4 °C for up to one month. Prior to inoculation, the detached roots were surface sterilized with 75% ethanol for 10 min, followed by 5% bleach for 5 min, and then thoroughly washed with dsH_2O. Approximately 1.5 mm wide and 9 mm deep holes were created on the roots using a sterilized needle, and then 15 µL of spore suspension were added into each hole. Similar holes were created in control roots (negative control) and treated similarly with only dsH_2O. After incubation, the roots were placed on sterile, wet paper filters in petri dishes and incubated at 22 °C for 12 days in the dark. Then lesion areas were assessed by tracing the rotted area on acetate sheets, scanning the sheets, and quantifying the areas using ImageJ software version 1.22 (imagej.nih.gov, accessed on June 2018). Five replicate lesions were measured at 12 dpi (days post-inoculation). Data were compared by the analysis of variance (ANOVA) using Minitab version 16 (www.minitab.com, accessed on 14 May 2018), and means were compared using Fisher's LSD Test at $p = 0.05$.

2.4. Genome Sequencing, Assembly and Gene Prediction

DNA from 600 mg of mycelia of the *I. mors-panacis* and *I. robusta* isolates (Table 1) was extracted as previously described. The DNA was submitted to Génome Québec/McGill University Innovation Centre (www.genomequebec.com, accessed on 30 May 2018) for 150 bp paired-end sequencing on the Illumina HiSeq 2500 platform (Illumina, San Diego, CA, USA) for three isolates (IMP.ND4Z15, IMP.RD3U14-5, IMP.RR3A14-1) and the Illumina HiSeq X Ten (Illumina, San Diego, CA, USA) for the remaining isolates. The raw sequenced reads were assembled into contigs and scaffolds using Velvet (www.ebi.ac.uk/~zerbino/velvet) accessed on 14 May 2018, SOAPdenovo (soapdenovo2.sourceforge.net) accessed on 21 May 2018, and ABySS (www.bcgsc.ca/platform/bioinfo/software/abyss) accessed on 28 May 2018 with odd-value k-mers ranging from 31 to 101. The assembly with the highest weighted median average scaffold length (N50) from among the three programs was selected for further analysis. The N50 value indicates that a scaffold of a certain length had 50% of all the sequenced bases in shorter scaffolds and 50% in larger scaffolds. The L50 value, which is defined as the count of the smallest number of contigs whose

length sum makes up half of the genome size, was determined using assemblathon_stats.pl (github.com/ucdavis-bioinformatics/assemblathon2-analysis) accessed on 11 June 2018.

Table 1. Identification and description of the *Ilyonectria mors-panacis* (IMP) and *I. robusta* (IR) isolates used in this study. All isolates were obtained from infected roots of *P. quinquefolius*, except for IR.DAOM139398 from *Prunus cerasus* cv. Montmorency and PMI-82 from *Populus deltoides*. Species identification was based on the histone H3 sequence as per Cabral et al. [4].

Isolate Code	Field Type [B]	Symptoms	Location	Year Isolated
IR.NR1BC16-1 [C]	N	Rusty root	Summerland, BC	2016
IR.ND1BC16-2 [C]	N	Black-brown lesion	Summerland, BC	2016
IR.NR2BC16-4 [C]	N	Rusty root	Summerland, BC	2016
IR.DAOM139398 [E]	Cherry orchard	ND	Georgian Bay, ON	-
IMP.ND3P14-1A	N	Black-brown lesion	St. Williams, ON	2016
IMP.ND3P14-3 [D]	N	Black-brown lesion	Lynedoch, ON	2014
IMP.ND3A16-1 [D]	N	Black-brown lesion	Delhi, ON	2016
IMP.ND4Z15 [D]	N	Black-brown lesion	Simcoe, ON	2015
IMP.ND3A16-2 [D]	N	Black-brown lesion	Delhi, ON	2016
IMP.ND3P14-1 [D]	N	Black-brown lesion	Lynedoch, ON	2014
IMP.RD3U14-8 [D]	R	Black-brown lesion	Scotland, ON	2014
IMP.RR3A14-1 [D]	R	Black-brown lesion and rusty root	Delhi, ON	2014
IMP.RD3U14-5 [D]	R	Black-brown lesion	Scotland, ON	2014
IMP.K112 [F]	ND	ND	Kamloops, BC	2006
IMP.DAOM226727 [G]	ND	ND	Delhi, ON	1996
IMP.DAOM226729	ND	ND	Delhi, ON	1935
I. europaea PMI-82 [A]	Poplar forest	ND	ND	-

[A] The genome of *I. europaea* PMI-82 was obtained from genome.jgi.doe.gov/Ilysp1/Ilysp1.home.html accessed on 11 June 2018. [B] R = Replant soil, N = Non-replant, ND = Not determined. [C] Jesse Macdonald, Agriculture & Agri-Food Canada. [D] Amy Fang Shi, Ontario Ginseng Growers Association. [E] S.J. Hughes, Agriculture & Agri-Food Canada. [F] Zamir Punja, Simon Fraser University. [G] Richard D. Reeleder, Agriculture & Agri-Food Canada.

The gene sets for each genome were predicted using AUGUSTUS 3.3.1 (github.com/Gaius-Augustus/Augustus accessed on 11 June 2018) using *Fusarium graminearum* as the model organism. Reciprocal comparisons of the genomes were made using standalone BLASTN with the BLAST v2.6.0+ suite [24]. The e-value cut-off was 1×10^{-3}, and the output format was set to tabular format. The genome of an isolate of *Ilyonectria europaea* was obtained from mycocosm.jgi.doe.gov/Ilysp1/Ilysp1.home.html accessed on 11 June 2018, and was included as a non-pathogen of ginseng as it had been isolated from *Populus deltoides* and has not been reported as a pathogen of ginseng [4]. To assess the completeness of the *Ilyonectria* genome assemblies, the presence or absence of highly conserved fungal genes was assessed with BUSCO 5.4.4 using the sordariomycetes_odb10 lineage dataset [25].

2.5. Total Predicted Gene Analysis

AUGUSTUS 3.3.1 was used to predict genes that were then aligned by MUSCLE 3.8.31. An unrooted maximum likelihood dendrogram was created using RAxML [26] (raxmlHPC-PTHREADS-AVX2 -s $inFile -n $outFile -w $outDir -f a -m PROTGAMMAWAGF -p 39543872 -x 15214 -# 1000 -T 4), and viewed in MEGA6 (www.megasoftware.net) accessed on 15 July 2018 with 1000 bootstrap replications shown as percentages at the nodes. The percent identity of all predicted genes in comparisons between genomes was determined by obtaining the BLASTN best reciprocal hit (RBH), thus obtaining the closest homolog for each predicted gene among the isolates. Then a super-matrix composed of the percent identity for each subject genome relative to each query genome was produced to obtain the summed nucleotide identity between each query and subject genome, followed by dividing by the summed alignment lengths in the self-hit query genome. Where a homolog was absent from any pairwise comparison, it contributed a null value and did not form part of the average pairwise distance. A tree was constructed with R (www.R-project.org) accessed

on 15 July 2018 using the package "ape" (Analyses of Phylogenetics and Evolution) with the Neighbour-Joining (NJ) algorithm [27].

2.6. Secretome Analysis

Secreted proteins were predicted using SignalP 4.1F (services.healthtech.dtu.dk/services/SignalP-4.1) accessed on 27 August 2018 with the default cut-off for the presence of the signal peptide (classical secretion) and SecretomeP 1.0H (services.healthtech.dtu.dk/services/SecretomeP-1.0) accessed on 27 August 2018 with the minimum cut-off of NN-score $\geq$0.50 for non-classical secreted proteins. Small secreted proteins (SSPs) had sequence lengths of $\leq$300 aa and did not have a significant match to a longer protein through reciprocal BLASTP. Cysteine residues were predicted using Pepstats from the EMBOSS 6.6.0 package (emboss.sourceforge.net/download) accessed August 2018. The SSPs were then categorized as either small secreted non-cysteine-rich (SSNPs, cysteine < 4) or small secreted cysteine-rich (SSCPs, cysteine $\geq$ 4). Secreted CAZymes were predicted based on domain searches using the HMMER profile (release 7.0) obtained from dbCAN (www.cazy.org/) accessed on 15 September 2018 with the script provided by dbCAN. Secreted proteases were predicted using BLASTP against the protein database from MEROPS release 12.0 (www.ebi.ac.uk/merops/) accessed on 17 September 2018. Secreted lipases were predicted using the HMMER profiles obtained from the Lipase Engineering Database release 3.0 (LED; www.led.uni-stuttgart.de/) accessed on 22 October 2018. The remaining predicted secreted proteins were divided into annotated or hypothetical/unknown proteins. A reciprocal BLASTP was used among the predicted proteins in each category, after which a distance matrix was generated and a neighbor-joining tree was produced. A homolog that was absent from any pairwise comparison contributed a null value and did not form part of the average pairwise distance. Data were compared by the analysis of variance (ANOVA) using R version 4.1.2, and comparison of means was done using Fisher's LSD Test, both at $p = 0.05$.

Cladograms were also created for the homologs (cut-off e-value of 1×10^{-5} in BLASTP) of the SSNP aa (amino acid) sequence matching the *Fusarium oxysporum* cone-rod homeobox effector (CRX1) (ALQ80856.1), which was correlated with virulence to onions [28], and for the SSCP aa sequence matching the *F. oxysporum* secreted in Xylem 6 effector (SIX6) (ACY39286.1), which was essential for virulence to tomato [29].

2.7. Non-Secretome Analysis

Searches in the genomes were made using the aa sequences of the *Aspergillus fumigatus* triacetylfusarinine C siderophore biosynthesis protein, L-ornithine N^5-oxygenase (SidA) (AAX40989.1) related to virulence [30], the *Alternaria jesenskae* branched-chain amino acid aminotransferase (TOXF) (AGQ43605.1) related to production of HC toxin [31], the *Botrytis cinerea* avenacinase (Sap1) (CAB61489.1) involved in degradation of the antimicrobial saponin avenacin [32], and the *Fusarium graminearum* mating type proteins MAT-1-1-3 (AAG42812.1) and MAT-1-2-1 (AAG42810.1) regulating sexual compatibility [33]. The predicted proteins were used as queries in a BLASTP search with a cut-off e-value of 1×10^{-5}.

3. Results

3.1. Histone H3 Sequencing

Based on histone H3 sequence, 11 isolates from Ontario were identified as *I. mors-panacis* and one as *I. robusta*, whereas one isolate from British Columbia was identified as *I. mors-panacis* and three as *I. robusta* (Table 1). Three isolates were from ginseng roots in replant soil, all from Ontario, and 10 were from ginseng roots in non-replant soil from both Ontario and British Columbia. This included the Ontario isolate that was from cherry roots in a cherry orchard, which was considered non-replant soil as ginseng had never been grown in it.

3.2. Growth Rate and Virulence

The growth rates on PDA varied considerably between the isolates, ranging from 0.25 to 0.62 cm/day (Table 2). However, the average growth rate of the 4 *I. robusta* isolates (0.59 cm/day) was significantly higher than the average for the 12 *I. mors-panacis* isolates (0.29 cm/day). In contrast, the average growth rate of *I. mors-panacis* isolates from roots in replanted soil (0.26 cm/day) was not significantly different from those from roots in non-replanted soil (0.32 cm/day).

Table 2. *Ilyonectria mors-panacis* (IMP) and *I. robusta* (IR) isolates (Table 1) growth rates in culture and lesion size produced on ginseng roots. Growth rates were measured on PDA after 12 days in dark at 22 °C. Lesion sizes produced by IMP and IR isolates were measured at 12 dpi (day post inoculation) on wounded roots inoculated with spore suspension (106 spores/mL in dsH_2O) from 4 week-old cultures grown on V8 media at 22 °C in the dark.

Isolate	Growth Rate (cm/day) [A]	Lesion Size (cm^2) [A]
IR.NR1BC16-1	0.63 ^{a}	0.18 ^{d}
IR.ND1BC16-2	0.61 ^{a}	0.14 ^{ef}
IR.NR2BC16-4	0.58 ^{ab}	0.13 ^{ef}
IR.DAOM139398	0.52 ^{c}	0.18 ^{d}
IMP.ND3P14-1A	0.41 ^{e}	0.23 ^{b}
IMP.ND3P14-3	0.43 ^{de}	0.09 ^{g}
IMP.ND3A16-1	0.25 ^{h}	0.30 ^{a}
IMP.ND4Z15	0.30 ^{fg}	0.20 ^{cd}
IMP.ND3A16-2	0.25 ^{h}	0.22 ^{b}
IMP.ND3P14-1	0.48 ^{cd}	0.18 ^{d}
IMP.RD3U14-8	0.27 ^{gh}	0.09 ^{g}
IMP.RR3A14-1	0.27 ^{gh}	0.17 ^{d}
IMP.RD3U14-5	0.26 ^{gh}	0.21 ^{bc}
IMP.K112	0.53 ^{bc}	0.14 ^{e}
IMP.DAOM226727	0.34 ^{f}	0.14 ^{ef}
IMP.DAOM226729	0.43 ^{de}	0.12 ^{f}

[A] Means followed by a lower-case letter in common are not significantly different according to LSD at $p = 0.05$.

Several isolates of *I. mors-panacis* (IMP.ND3P14-1A, IMP.ND3A16-1, IMP.ND3A16-2, and IMP.RD3U14-5) were significantly more virulent than any of the *I. robusta* isolates (Table 2). However, the average root lesion size produced by the *I. robusta* isolates was 0.16 cm^2, which was not significantly different from that produced by *the I. mors-panacis* isolates at 0.17 cm^2. The average root lesion size produced by *I. mors-panacis* isolates from roots in non-replant soil (0.20 cm^2) was not significantly different from that produced by *I. mors-panacis* isolates collected from roots in replant soil (0.16 cm^2). No significant relationships were observed between root lesion size and growth rate on PDA (Figure S1).

3.3. Genomic Sequencing and Assembly Quality

Excluding *I. europeae,* which was not sequenced and assembled in this study, the average number of scaffolds for the assembled *Ilyonectria* genomes was 5790, the average N50 value was 586,273, and the average L50 value was 64 (Table 3). Excluding *I. europeae*, an average of 98.7% of the 3817 BUSCO genes in the sordariomycetes_odb10 database were present as complete sequences in the *Ilyonectria* assemblies, and an additional 0.3% were present as fragmented copies (Table 3). Only an average of 1.0% of the genes were missing in the assemblies. These results indicate that the *Ilyonectria* assemblies were of high completeness. The genomes (Table 4) are available through NCBI, listed under BioProject PRJNA885578.

Table 3. Quality parameters of the genomes sequenced for *I. mors-panacis* (IMP), *I. robusta* (IR) and *I. europaea*.

					BUSCO (3817 Groups in Sardariomycetes_odb10)				
Isolate [A]	**WGS Accession**	**Scaffolds**	**N50**	**L50**	**Complete**	**Single-Copy**	**Duplicated**	**Fragmented**	**Missing**
IR.NR1BC16-1	JAQYTY000000000	2652	1,630,377	67	3764	3730	34	7	46
IR.ND1BC16-2	JAQYTZ000000000	10,371	899,178	67	3766	3713	53	6	45
IR.NR2BC16-4	JAQYTX000000000	1549	1,566,478	67	3763	3728	35	6	48
IR.DAOM139398	JAQYUA000000000	1690	1,976,210	67	3767	3737	30	6	44
IMP.ND3P14-1A	JAQYUG000000000	8384	270,784	67	3760	3731	37	11	38
IMP.ND3P14-3	JAQYUF000000000	4472	303,308	64	3768	3729	39	12	37
IMP.ND3A16-1	JAQYUJ000000000	7456	371,676	54	3769	3732	37	12	36
IMP.ND4Z15	JAQYUE000000000	4256	179,452	67	3766	3730	36	13	38
IMP.ND3A16-2	JAQYUI000000000	8029	285,004	66	3768	3729	39	12	37
IMP.ND3P14-1	JAQYUH000000000	8662	291,290	62	3768	3730	38	11	38
IMP.RD3U14-8	JAQYUC000000000	7651	334,621	67	3767	3730	37	13	37
IMP.RR3A14-1	JAQYUB000000000	3907	178,193	67	3766	3727	39	14	37
IMP.RD3U14-5	JAQYUD000000000	3372	178,475	67	3767	3728	39	13	37
IMP.K112	JAQYUK000000000	4268	278,127	61	3768	3728	40	13	36
IMP. DAOM226727	JAQYUM000000000	8002	284,075	63	3769	3731	38	12	36
IMP. DAOM226729	JAQYUL000000000	7918	353,126	58	3769	3730	39	13	35
I. europaea PMI-82	N/A	325	327,392	9	3763	3703	60	6	48

[A] The *I. europaea* genome accession (JGI: 1006312) is for the JGI Genome portal (genome.jgi.doe.gov/portal/) accessed on 11 June 2018, while the other genome accessions are for NCBI Genome (www.ncbi.nlm.nih.gov/genome/) accessed on 11 June 2018. All other *Ilyonectria* genome accessions can be found through NCBI's BioProject with the accession PRJNA885578.

Table 4. Average genome size, number of predicted genes and GC content of *I. mors-panacis*, *I. robusta* and *I. europaea* isolates (Table 1).

Isolate [A]	**Genome Size (Mbp)** [B]	**Predicted Genes** [B]	**GC Content** [B]
I. robusta	59.2 [b]	17,603.5 [b]	50.1% [a]
I. mors-panacis type 1	65.02 [a]	18,183.4 [ab]	48.92% [b]
I. mors-panacis type 2	65.04 [a]	18,370.2 [a]	48.98% [b]
I. europaea PMI-82	63.7	19,307	51.13%

[A] The *I. europaea* genome accession (JGI: 1006312) is for JGI Genome portal (genome.jgi.doe.gov/portal/) accessed on 11 June 2018, while the other genome accessions are for NCBI Genome (www.ncbi.nlm.nih.gov/genome/) accessed on 11 June 2018. All other *Ilyonectria* genome accessions can be found through NCBI's BioProject with the accession PRJNA885578. [B] Means followed by a lower-case letter in common are not significantly different according to LSD at $p = 0.05$.

3.4. Total Predicted Genes of the Ilyonectria Isolates

A tree of the nucleotide (nt) sequences of the total predicted genes of the genomes of the *Ilyonectria* isolates showed two distinct clades comprising a cluster of all *I. mors-panacis* isolates and another cluster of all *I. robusta* isolates, which were closely related to the *I. europaea* isolate (Figure 1). The tree also showed that *I. mors-panacis* isolates were divided into two distinct groups. One group was designated type 1, containing seven *I. mors-panacis* isolates, and the other group was designated type 2, containing five *I. mors-panacis* isolates. Bootstrap support was 100% for the node between *I. robusta* and *I. mors-panacis* and 96% for the separation between types 1 and 2 *I. mors-panacis*. Type 1 included isolates from roots in non-replant soil (IMP.ND3A16-1, IMP.ND3A16-2, IMP.ND3P14-1, and IMP.ND3P14-1A), replant soil (IMP.RD3U14-8), and unknown soil (IMP.DAOM226729

and IMP.DAOM226727). Type 2 also included isolates from roots in non-replant soil (IMP.ND3P14-3 and IMP.ND4Z15), replant soil (IMP.RD3U14-5 and IMP.RR3A14-1), and unknown soil (IMP.K112). Both types contained isolates from the same area of southern Ontario, while the one isolate of *I. mors-panacis* from British Columbia belonged to type 2. No significant differences in average growth rate or lesion size in roots were observed between type 1 and type 2 isolates (data not shown).

Figure 1. Relatedness based on nt sequences of total predicted genes in the genomes of *I. mors-panacis* (IMP), *I. robusta* (IR), and *I. europaea* isolates (Table 1) and identification of type 1 and type 2 IMP isolates. An unrooted neighbor-joining dendrogram was created using R and viewed by MEGA6 based on a similarity matrix of the percent identity obtained from the reciprocal best hit BLASTN results between the AUGUSTUS predicted genes (nt) with a 1000 bootstrap replications shown as a percent. Scale bar indicates the distance based on the average expected differences in the sequences. Numbers 1 and 2 refer to IMP types 1 and 2.

3.5. Genomic Comparisons of the Ilyonectria Isolates

The average genome size of *I. robusta* isolates was significantly smaller than that of type 1 and type 2 *I. mors-panacis* isolates (Table 4). However, the average number of total predicted genes of the *I. robusta* isolates was not significantly different than that of type 1 *I. mors-panacis* isolates, although it was significantly lower than that of type 2 *I. mors-panacis*. The average GC content of the *I. robusta* isolates was significantly higher than the GC content of the type 1 and 2 *I. mors-panacis* isolates. By comparison, the *I. europaea* isolate had a genome size between that of *I. robusta* and *I. mors-panacis* but a higher number of predicted genes and GC content relative to that of *I. robusta* and *I. mors-panacis*.

The average number of total predicted non-secreted proteins and secreted proteins per isolate was not significantly different between the *I. robusta* and type 1 and 2 *I. mors-panacis* isolates (Table 5). The predicted proteins of the secretome of the isolates were divided into seven categories (Table 5). For *I. robusta* and *I. mors-panacis* genomes in this study, the secretomes were on average categorized as 14.7% SSNPs, 7.7% SSCPs, 8.1% oxidoreductases, 7.4% CAZymes, 6.6% proteases, and 4.5% lipases. In addition, an average of 32.1% of the secretomes were classified as other annotated proteins, and the remaining 22.0% were classified as hypothetical/unknown proteins. The only significant difference in the number of predicted genes in those categories was a higher number of SSNPs and SSCPs in type 1

and 2 *I. mors-panacis* isolates compared to *I. robusta* isolates. By comparison, the *I. europaea* isolate had fewer hypothetical proteins and higher numbers in other categories.

Table 5. Average number of total non-secreted and secreted predicted proteins and groups in the predicted secretome (small non-cysteine-rich proteins (SSNPs), small cysteine-rich proteins (SSCPs), CAZymes, proteases, lipases, other annotated proteins, and hypothetical/unknown proteins) of *I. mors-panacis*, *I. robusta* and *I. europaea* isolates (Table 1).

Isolate	Total Non-Secreted Proteins	Total Secreted Proteins	Secreted SSNPs	Secreted SSCPs	Secreted CAZymes	Secreted Proteases	Secreted Lipases	Other Secreted Annotated Proteins	Secreted Hypothetical/Unknown Proteins
I. robusta	8869 [a]	8736 [a]	1269 [b]	677 [b]	673 [a]	585 [a]	414 [a]	3013 [a]	1917 [a]
I. mors-panacis type 1	8945 [a]	9240 [a]	1370 [a]	698 [a]	669 [a]	595 [a]	409 [a]	2622 [a]	1876 [a]
I. mors-panacis type 2	9180 [a]	9191 [a]	1372 [a]	705 [a]	666 [a]	595 [a]	410 [a]	3075 [a]	2196 [a]
I. europaea PMI-82	9474	9834	2386	1159	782	654	504	3077	1613

Means followed by a lower-case letter in common are not significantly different according to LSD at $p = 0.05$.

3.6. Secretome of the Ilyonectria Isolates

For the neighbor-joining dendrogram based on gene sequences from the total predicted secretome of each *Ilyonectria* isolate, there were two distinct clades comprising a cluster of all *I. mors-panacis* isolates and the other cluster of *I. robusta* isolates, which was closely related to the *I. europaea* isolate (Figure 2). The *I. mors-panacis* isolates were divided into types 1 and 2, as was observed with the dendrogram based on predicted sequences of all genes in each genome (Figure 1). Bootstrap support was 100% for the node between *I. robusta* and *I. mors-panacis* and 96% for the separation between types 1 and 2 of *I. mors-panacis*.

Figure 2. Relatedness based on aa sequences of total predicted secretomes of the *I. mors-panacis* (IMP), *I. robusta* (IR), and *I. europaea* isolates (Table 1). An unrooted neighbor-joining dendrogram was created using R based on a similarity matrix of the percent identity obtained from reciprocal best hit BLASTP between the AUGUSTUS predicted proteins in each genome and viewed in MEGA6. Bootstrap values based on 1000 replicates are shown as a percent. Scale bar is based on percent identity of the reciprocal matches. Numbers 1 and 2 refer to IMP types 1 and 2.

For the dendrogram based on the predicted SSNP aa sequences, the clustering matched that based on the total secretome, with *I. robusta* being distinct from the type 1 and 2 *I. mors-panacis* isolates, which were distinguishable from each other (Figure 3). Bootstrap support was 91% for the node between type 1 and type 2 *I. mors-panacis* isolates. For the dendrogram based on predicted SSCP aa sequences, clustering was similar to that of the total secretome, except that clustering of the type 1 and type 2 *I. mors-panacis* isolates was not as distinct (Figure 4). For the node between type 1 and type 2 isolates, bootstrap support was 99%. For the dendrogram based on predicted secreted protease aa sequences,

clustering was similar to the total secretome, except that the clustering of types 1 and 2 *I. mors-panacis* isolates was less distinct (Figure 5). For the node between types 1 and 2, *I. mors-panacis*, bootstrap support was 77%. For the dendrogram based on predicted secreted CAZyme and lipase aa sequences, the clustering of *I. robusta* and *I. mors-panacis* was similar to that of the total secretome, but the *I. mors-panacis* isolates no longer showed a division between type 1 and type 2 isolates (Figures S2 and S3). Bootstrap support for the node between *I. robusta* and *I. mors-panacis* was 100% for SSNPs, SSCPs, and secreted proteases, CAZymes, and lipases.

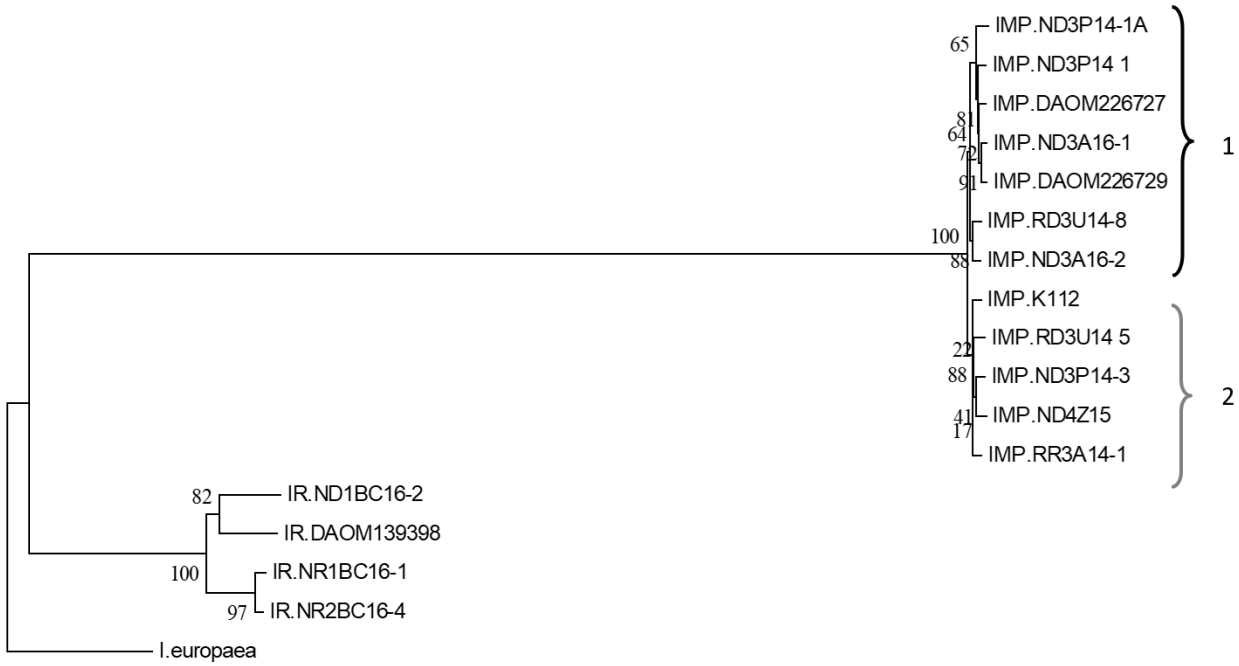

Figure 3. Relatedness based on aa sequences of predicted SSNPs in the genomes of *I. mors-panacis* (IMP), *I. robusta* (IR), and *I. europaea* isolates (Table 1). An unrooted neighbor-joining dendrogram was created using R and viewed by MEGA6 based on a similarity matrix of the percent identity obtained from reciprocal best-hit BLASTP between the AUGUSTUS predicted proteins in each genome. Bootstrap values based on 1000 replicates are shown as a percent. Scale bar is based on percent identity of the reciprocal matches. Numbers 1 and 2 refer to IMP types 1 and 2.

Among the SSNPs, there was only one aa predicted sequence matching a known fungal effector, which was the cone-rod homeobox effector, CRX1, of *F. oxysporum*. Each *I. robusta* genome contained one copy, except for IR.ND1BC16-2, which lacked a copy, while each *I. mors-panacis* genome contained two copies (Figure S4). Cluster 1 contained only *I. mors-panacis* sequences that were all identical, while cluster 2 contained both *I. robusta* and *I. mors-panacis* sequences. Differences between *I. mors-panacis* sequences in cluster 2 were not related to the division of *I. mors-panacis* into types 1 and 2.

Among the SSCPs, there was only one predicted aa sequence matching a known fungal effector, which was the Secreted in Xylem 6 effector, SIX6, of *F. oxysporum*. All the isolates of *I. robusta* contained one copy, while all isolates of *I. mors-panacis* lacked a copy (Figure S5). The predicted SIX6 proteins from *I. robusta* isolates all had identical sequences.

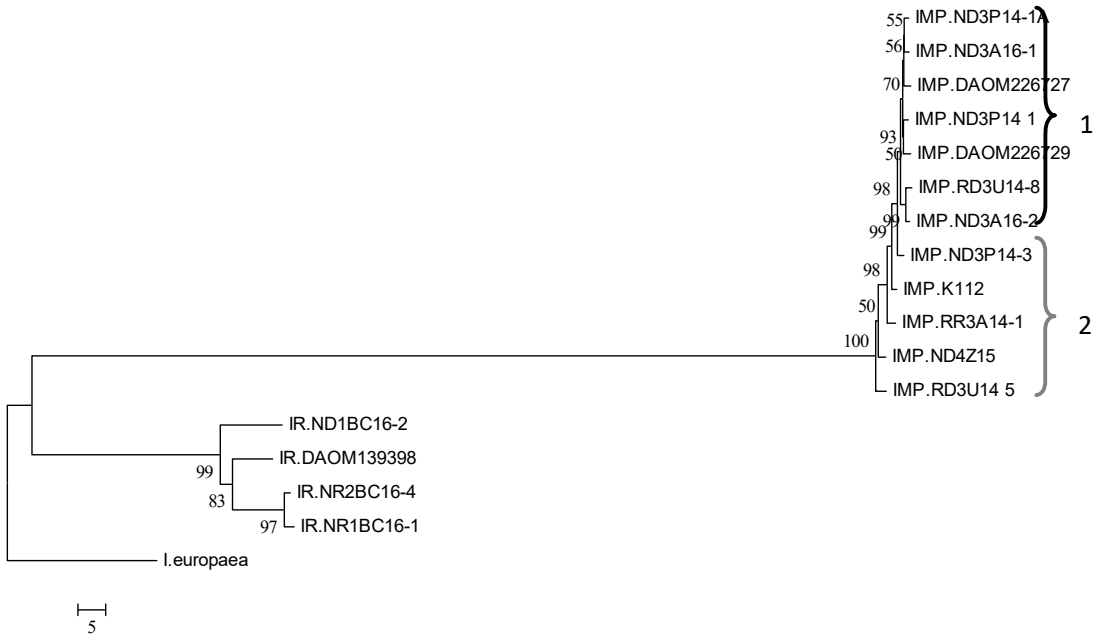

Figure 4. Relatedness based on aa sequences of predicted SSCPs in the genomes of *I. mors-panacis* (IMP), *I. robusta* (IR), and *I. europaea* isolates (Table 1). An unrooted neighbor-joining dendrogram was created using R and viewed by MEGA6 based on a similarity matrix of the percent identity obtained from reciprocal best-hit BLASTP between the AUGUSTUS predicted proteins in each genome. Bootstrap values based on 1000 replicates are shown as a percent. Scale bar is based on percent identity of the reciprocal matches. Numbers 1 and 2 refer to IMP types 1 and 2.

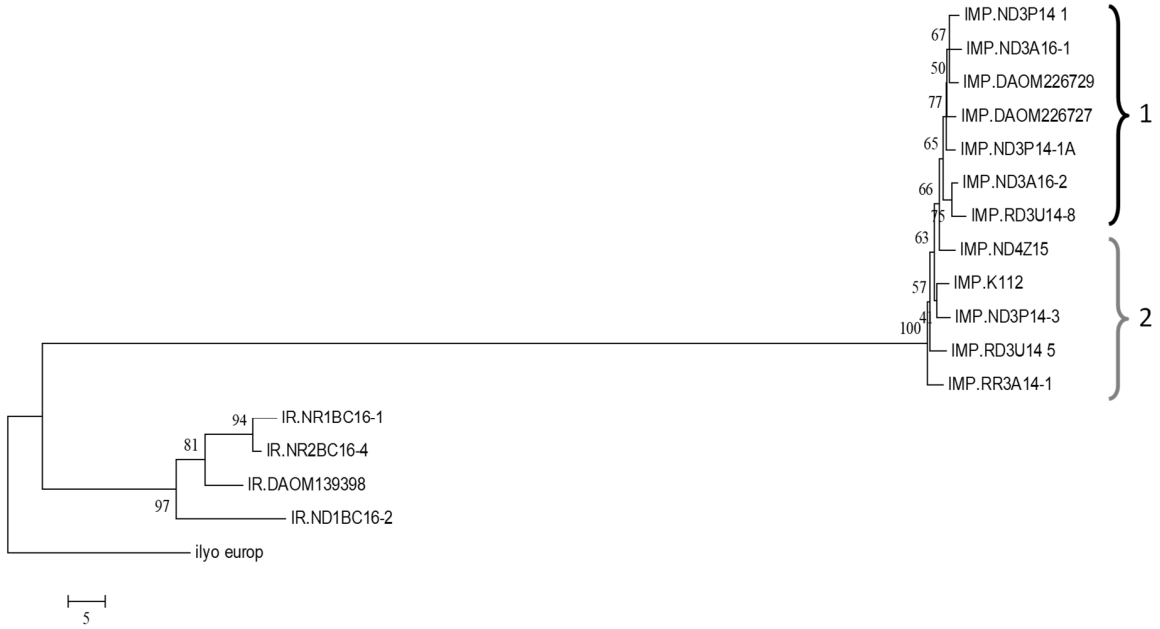

Figure 5. Relatedness based on aa sequences of predicted secreted proteases in the genomes of *I. mors-panacis* (IMP), *I. robusta* (IR), and *I. europaea* isolates (Table 1). An unrooted neighbor-joining dendrogram was created using R and viewed by MEGA6 based on a similarity matrix of the percent identity obtained from reciprocal best-hit BLASTP between the AUGUSTUS predicted proteins in each genome. Bootstrap values, based on 1000 replicates are shown as a percent. Scale bar is based on percent identity of the reciprocal matches. Numbers 1 and 2 refer to IMP types 1 and 2.

3.7. Non-Secretome of the Ilyonectria Isolates

A neighbor-joining dendrogram based on the aa sequences of the total predicted non-secretome also showed a cluster of all the *I. robusta* isolates placed close to the *I. europaea* isolate and two sub-clusters of *I. mors-panacis* isolates related to the division into type 1 and type 2 isolates (Figure 6). For the node between *I. robusta* and *I. mors-panacis*, bootstrap support was 79%, while between types 1 and 2, it was 77%. Comparisons were made for several predicted non-secretome proteins, which may be related to virulence or sexual development.

For proteins possibly related to virulence, the predicted aa sequences matching the triacetylfusarinine C siderophore biosynthesis enzyme of *A. fumigatus* were found in the non-secretomes, with one copy in the genome of each *I. europaea*, *I. mors-panacis,* and *I. robusta* isolate (Figure S6). All the aa sequences were identical among the *I. robusta* and the *I. mors-panacis* isolates. Predicted aa sequences matching the HC-toxin branched-chain amino acid aminotransferase enzyme of *A. jesenskae* were found with one copy in the genome of each *I. europaea* and *I. robusta* isolate and three copies in the genome of each *I. mors-panacis* isolate (Figure S7). Cluster 1 contained sequences from *I. robusta* and *I. europaea*, while clusters 2, 3, and 4 contained sequences from *I. mors-panacis*, which were all identical within each cluster. Predicted aa sequences matching the avenacinase enzyme of *B. cinerea* were found with two copies in the genomes of each *I. europaea* and *I. robusta* isolate and three copies in the genomes of each *I. mors-panacis* isolate (Figure S8). Cluster 1 contained sequences from *I. mors-panacis* and *I. europaea*, and cluster 2 contained sequences from *I. robusta*, *I. mors-panacis,* and *I. europaea*. Clusters 3 and 4 contained sequences from *I. mors-panacis* and *I. robusta*, respectively. All the sequences within each cluster from the same species were identical except for those of *I. robusta* in cluster 4. Thus, there was no relationship between the clustering of any of those predicted proteins and the division of type 1 and type 2 *I. mors-panacis*.

Figure 6. Relatedness based on aa sequences of total predicted non-secretomes in the genomes of the *I. mors-panacis* (IMP), *I. robusta* (IR), and *I. europaea* isolates (Table 1). An unrooted neighbor-joining dendrogram was created using R and viewed by MEGA6 based on a similarity matrix of the percent identity obtained from reciprocal best-hit BLASTP between the AUGUSTUS predicted proteins in each genome. Bootstrap values based on 1000 replicates are shown as a percent. Scale bar is based on percent identity of the reciprocal matches. Numbers 1 and 2 refer to MP types 1 and 2.

For proteins related to sexual development, predicted aa sequences matching mating-type proteins of *F. graminearum* were also found in the genomes. For the MAT1-2-1 sequence, there were three copies in the genome of each *I. europaea*, *I. robusta,* and *I. mors-panacis* isolate (Figure S9). Clusters 1, 2, and 3 each contained one set of sequences from *I. robusta*, *I. mors-panacis,* and *I. europaea*. The *I. mors-panacis* sequences were identical within each cluster, whereas the *I. robusta* sequences were identical within clusters 1 and 3 but not cluster 2. For the MAT1-1-3 sequence, there were two copies in the genome of each *I. europaea*, *I. robusta,* and *I. mors-panacis* isolate (Figure S10). Cluster 1 contained one set of sequences from *I. europaea*, all the *I. robusta* isolates except DAOM139398, and all the *I. mors-panacis* isolates, with each species having identical sequences. Cluster 2 contained sequences from each of the three species, with each species having identical sequences except for *I. robusta,* which contained two different sequences for isolate DAOM139398. As the sequences were identical for all *I. mors-panacis* isolates within each cluster, no relationship was observed between the MAT1-2-1 and MAT1-1-3 sequences and the division between type 1 and type 2 *I. mors-panacis*.

4. Discussion

While there was a wide range of growth rates in culture, the four isolates of *I. robusta* grew on average faster on PDA than the twelve isolates of *I. mors-panacis*, suggesting stronger saprophytic ability. Farh et al. [34] noted that the relative growth rate on V8 media containing ginsenosides was higher for *I. robusta* than for *I. mors-panacis*, which was related to their ability to metabolize ginsenosides, but they did not report the growth rates on V8 media not amended with ginsenosides. The faster growth rate in PDA by *I. robusta* compared to *I. mors-panacis* may be due to a better ability to access or transport nutrients, a higher saprophytic metabolic rate, or some other factor.

There are several reports that *I. mors-panacis* is more virulent against ginseng compared to other *Ilyonectria* species. Farh et al. [34] showed that disease severity on *P. ginseng* roots grown in soil infested with isolates of *I. mors-panacis* was significantly higher than that of isolates of *I. robusta* or isolates of *I. leucospermi* from *P. ginseng* roots. Based on disease rating and stand counts of *P. quinquefolius* seedlings in inoculated soil, Seifert et al. [35] reported that four isolates of *C. destructans* f. sp. *Panacis* (i.e., *I. mors-panacis*) were more virulent than three other *C. destructans* isolates, which were likely one of the other *Ilyonectria* species pathogenic to ginseng [4]. However, in this study, the average lesion size created by the *I. robusta* and *I. mors-panacis* isolates was not significantly different using detached *P. quinquefolius* roots inoculated with conidia. There was a range of virulence for isolates of both *I. mors-panacis* and *I. robusta,* with some *I. mors-panacis* isolates (IMP.RD U14-8 and IMP.ND3P14-3) having lower virulence than any *I. robusta* isolate tested. Although the *I. robusta* isolates had a similar average virulence as the *I. mors-panacis* isolates in this study, *I. robusta* does not appear to be a common pathogen of ginseng, at least in Ontario. No isolates of *I. robusta* were obtained from infected ginseng roots compared to over 50 isolates of *I. mors-panacis* from surveys of commercial ginseng gardens in Ontario over the last 10 years (F. Shi, Ontario Ginseng Growers Association, personal communication).

A comparison of the nt sequences of all predicted genes showed clear differences between *I. mors-panacis* and *I. robusta*, which was as expected, but surprisingly also showed a division of the *I. mors-panacis* isolates into two types. In addition, sequence comparisons among the total non-secretome and total secretome, as well as the SSNP, SSCP, and protease components of the secretome, supported this division of *I. mors-panacis* types 1 and 2, which was unexpected as there are no previous reports of a division within *I. mors-panacis.* In contrast, *C. destructans* f. sp. *panacis* (i.e., *I. mors-panacis*) isolates from Ontario, Korea, and Japan were considered a monophyletic clade based on identical ITS and β-tubulin sequences [35]. Thus, one would have expected little variation among the genomes of the *I. mors-panacis* isolates. However, the biological significance of the division of *I. mors-panacis* into type 1 and type 2 isolates is unclear, as it was not clearly related to growth rates, virulence, or the geographical source of the isolates.

The genomes of 16 *Ilyonectria* isolates in this study ranged from 56.1 to 65.3 Mbp, and the average genome size of the *I. mors-panacis* isolates was significantly larger than the *I. robusta* isolates. However, there were no differences in average genome size between type 1 and type 2 isolates of *I. mors-panacis*. Zhu et al. [22] estimated a genome size of 61 Mbp for an isolate of *I. mors-panacis* from *P. notoginseng*, and Guan et al. [21] estimated a genome size of 58 Mbp for an isolate of *I. robusta* from *P. ginseng* roots. However, this is the first comparison of multiple *I. mors-panacis* and *I. robusta* isolates showing that there are consistent differences between the two species. Genome enlargement has been reported to be due to an increase in repeat sequences, such as a proliferation of transposable elements [36,37] or a dysfunctional repeat-induced mutation pathway [37]. It has been proposed that fungal plant pathogens with larger genomes can possibly adapt faster by producing virulent types able to combat the host's innate immune system [36]. Thus, the larger genome size of *I. mors-panacis* may be related to a greater potential for overcoming host resistance than that of *I. robusta*.

The total number of predicted genes per genome ranged from 17,256 to 19,307, which agrees with the 18,321 predicted genes for *I. mors-panacis* G3B [22] and the 17,752 predicted genes for *I. robusta* CD-56 [21]. However, there were no significant differences in the total number of predicted non-secreted or secreted genes between type 1 and type 2 *I. mors-panacis* compared to *I. robusta*. Although *I. mors-panacis* isolates had a larger genome, there was not a significant correlation between genome size and the number of predicted genes within the two species. This indicates that the differences may be due to variation in non-coding regions, such as intergenic DNA [38], microsatellites [39], and pseudogenes [40,41].

The average GC content was significantly higher in the *I. robusta* isolates than in the type 1 or 2 *I. mors-panacis* isolates in this study. The GC content previously reported for *I. robusta* CD-56 (49.3%) [21] was also higher than that reported for *I. mors-panacis* G3B (48.7%) [22], but this is the first report comparing multiple isolates. Differences in GC content between fungal isolates can reflect microsatellite density, with lower GC content indicating higher microsatellite density dominated by A/T-rich motifs produced by repeat-induced point mutations that can act as a defense against transposon propagation [42,43]. Thus, one possibility is that *I. robusta* has experienced greater repeat-induced point mutations than *I. mors-panacis.*

A comparison was also made for the approximately 9000 predicted proteins in the secretomes. The secretomes in plant pathogenic fungi are often studied because they are believed to be related to virulence with secreted enzymes such as plant cell-wall degrading enzymes, proteases, and saponin detoxifying enzymes [17–19], as well as secreted immunosuppressing effectors [16,20]. Among the SSCPs and SSNPs, two predicted protein sequences were found to match known fungal effectors, CRX1 and SIX6. CRX1 has been shown to correlate with the virulence of *F. oxysporum* during onion infection [28]. SIX6 is essential for the virulence of *F. oxysporum* during tomato infection [29]. CRX1 sequences were found in both species, but SIX6 sequences were absent in *I. mors-panacis*. Identical sequences were found in isolates differing in virulence, and further work is needed to determine if they have a role in virulence.

The non-secreted proteins of fungi are involved in a wide range of functions in primary and secondary metabolism and could be important for virulence. Some non-secreted proteins of *Ilyonectria* spp. have been proposed to be virulence factors. Siderophores in fungi are low-molecular-weight iron-chelating compounds produced as hydroxamates that can enhance pathogenicity and suppress the growth of other microorganisms [44]. The siderophore, N,N′,N″-triacetylfusarinine C, of *I. mors-panacis* was related to virulence based on its production by three isolates of *I. mors-panacis* virulent to ginseng, whereas no production was observed in two isolates of *Ilyonectria rufa* and an isolate of *Cylindrocarpon obtusisporum* that had low or no virulence to ginseng roots [45]. A homolog of the siderophore biosynthesis protein (L-ornithine N^5-oxygenase) from *Aspergillus fumigatus* [30] was found in the genomes of *I. robusta* and *I. mors-panacis* isolates in this study. They were identical within each species but different between species, and they were found in isolates

with a range of virulence. However, virulence could be related to the level of L-ornithine N^5-oxygenase expression.

The synthesis of cyclic peptides requires non-ribosomal peptide synthetases, such as the branched-chain amino acid aminotransferase TOXF, which acts in the biosynthesis of the HC toxin of *C. carbonum* [31,46]. TOXF is required for virulence and is unrelated to house-keeping versions of branched-chain amino acid aminotransferases [31]. The TOXF sequences from *I. robusta* were distinct from the TOXF sequences from the *I. mors-panacis* genomes, which occurred in the three clusters. It appears that *I. robusta* and *I. mors-panacis* produce different cyclic peptides, and one or more of them may be a cyclic peptide toxin. There were no aa sequence differences in the TOXF genes within isolates of *I. robusta* or *I. mors-panacis* differing in virulence, and thus further work is needed to determine if any of the putative cyclic peptides are involved in the virulence of ginseng. Ginsenosides are saponins that can have anti-fungal activity [47], and ginsenoside levels are relatively high in healthy ginseng roots [48], as well as induced in *P. ginseng* roots during infection by *I. robusta,* although suppressed by *I. mors-panacis* [49]. Farh et al. [34] reported that the ability to partially degrade protopanaxdiol-type ginsenosides in culture was a characteristic of *I. robusta* but not of *I. mors-panacis*. Both the *I. robusta* and *I. mors-panacis* isolates in this study contained sequences similar to the β-glucosidase avenacinase of *B. cinerea*, which reduces saponin toxicity by removing glucose from avenacin [32]. However, *I. robusta* and *I. mors-panacis* may differ in their ability to degrade saponins, as two types of sequences (clusters 1 and 3) were unique to *I. mors-panacis*, while one type of sequence (cluster 4) was unique to *I. robusta*. It is not known if any of these β-glucosidase avenacinase-like proteins are involved in ginsenoside metabolism.

Another element of the non-secretome examined was mating-type genes. Mating type proteins act as transcription factors related to mating and sexual development, and heterothallic fungi have genes for two different mating type proteins in different isolates, whereas homothallic fungi have both mating type protein genes within each isolate [50,51]. Sequences matching the MAT 1-1-3 and MAT 1-2-1 proteins of *F. graminearum* [33] were found in all isolates with copies of each in each genome, indicating that both species are homothallic [52]. As there were no sequence differences in MAT 1-1-3 and MAT 1-2-1 between type 1 and type 2 *I. mors-panacis* isolates, the division of *I. mors-panacis* into types 1 and 2 does not appear to be related to mating type.

One factor that could affect the results of this study is phylogenetic discordance, which can be caused by factors such as incomplete lineage sorting, lineage jumps in ancestral populations, and gene duplication and loss with lineage extinction [53]. For example, the results of this study comparing gene groupings could be affected by the loss of some related genes within only one type of *I. mors-panacis*. Therefore, a quantitatively biased method using the entire coding sequences or large groups of sequences may not always show the true lineage as differences. The supermatrix data dealt only with the overall quantitative data and did not take into account any differences, such as the loss of some of the genes. Future work is needed to examine this in more detail, such as by conducting sequence alignments for each individual gene category.

5. Conclusions

Both the *I. mors-panacis* and *I. robusta* isolates in this study showed variation in virulence; however, isolates of *I. mors-panacis* were not consistently more virulent than *I. robusta*. Nor was there any evidence that isolates from roots in replanted soil were more virulent than those from roots in non-replanted soil. While differences between the genomes of *I. mors-panacis* and *I. robusta* were expected, surprisingly, *I. mors-panacis* could be divided into two types based on the similarity of the nt sequences of the coding regions of the genomes as revealed in the dendrograms. These differences were also observed in dendrograms of the total non-secretome, total secretome, and several categories of the secretome, such as proteases, which could impact the virulence of the isolates. For example, the secreted proteases FoMep1 and FoSep1 of *Fusarium oxysporum* are important virulence factors that

degrade defense-related chitinases in tomatoes [54]. While the significance of the division of the *I. mors-panacis* isolates remains to be determined, there may be many impacts considering the wide range of secretome proteins that differ in the genomes of type 1 and type 2 *I. mors-panacis*. Future work is needed to assess their attributes.

Supplementary Materials: The following supporting information can be downloaded at: https://www.mdpi.com/article/10.3390/horticulturae9060713/s1, Figure S1. Relationship of *Ilyonectria* isolates (Table 1) based on growth rate on PDA for 12 days at 22 °C in the dark vs. root lesion size produced by the *Ilyonectria* isolate. Red crosses and blue circles indicate *I. robusta* and *I. mors-panacis* isolates, respectively. Figure S2. Relatedness based on aa sequences of predicted secreted CAZymes in the genomes of *I. mors-panacis* (IMP), *I. robusta* (IR), and *I. europaea* isolates (Table 1). An unrooted neighbor-joining dendrogram was created using R and viewed by MEGA6 based on a similarity matrix of the percent identity obtained from reciprocal best-hit BLASTP between the AUGUSTUS predicted proteins in each genome. Bootstrap values based on 1000 replicates are shown as a percent. The scale bar is based on the percent identity of the reciprocal matches. Numbers 1 and 2 refer to *I. mors-panacis* types 1 and 2. Figure S3. Relatedness based on aa sequences of secreted lipases in the genomes of *I. mors-panacis* (IMP), *I. robusta* (IR), and *I. europaea* isolates (Table 1). An unrooted neighbor-joining dendrogram was created using R and viewed by MEGA6 based on a similarity matrix of the percent identity obtained from reciprocal best-hit BLASTP between the AUGUSTUS predicted proteins in each genome. Bootstrap values based on 1000 replicates are shown as a percent. The scale bar is based on the percent identity of the reciprocal matches. Numbers 1 and 2 refer to IMP types 1 and 2. Figure S4. Relatedness based on aa sequences of the cone-rod homeobox effector, CRX1, of *I. mors-panacis* (IMP), *I. robusta* (IR), and *I. europaea* isolates (Table 1). The cladogram was created using RAxML and viewed by MEGA6. Bootstrap values based on 1000 replicates are shown as a percent. The scale bar is based on the difference in aa sequences per site. Clusters marked as 1 and 2 refer to copies 1 and 2 of the predicted genes found in one or more of the genomes. Figure S5. Relatedness based on aa sequences of the secreted in xylem 6 effector, SIX6, of *I. mors-panacis* (IMP), *I. robusta* (IR), and *I. europaea* isolates (Table 1). The cladogram was created using RAxML and viewed by MEGA6. The scale bar indicates the distance of the isolates from one another based on the average expected differences in the gene sequences per site. None of the *I. mors-panacis* isolates contained SIX6 proteins. The scale bar is based on the difference in aa sequences per site. Figure S6. Relatedness based on aa sequences of the triacetylfusarinine C siderophore biosynthesis enzyme, L-ornithine N^5-oxygenase, of *I. mors-panacis* (IMP), *I. robusta* (IR), and *I. europaea* isolates (Table 1). Triacetylfusarinine C siderophore biosynthesis proteins were identified based on BLASTP of the total predicted proteins of each genome using the protein sequence of *Aspergillus fumigatus* SidA (AAX40989.1) as a query. The cladogram was created using RAxML and viewed by MEGA6. Bootstrap values based on 1000 replicates are shown as a percent. The scale bar is based on the difference in aa sequences per site. Figure S7. Relatedness based on the aa sequences of the HC-toxin branched-chain amino acid aminotransferase, TOXF, protein of *I. mors-panacis* (IMP), *I. robusta* (IR), and *I. europaea* isolates (Table 1). HC-toxin branched-chain amino acid aminotransferases were identified based on BLASTP of the total predicted proteins of each genome using the TOXF homology protein sequence of *Alternaria jesenskae* (AGQ43605.1) as a query. The cladogram was created using RAxML and viewed by MEGA6. Bootstrap values based on 1000 replicates are shown as a percent. The scale bar is based on the difference in aa sequences per site. Clusters marked as 1, 2, 3, and 4 refer to copies 1, 2, 3, and 4 of the predicted genes found in one or more of the genomes. Figure S8. Relatedness based on the aa sequences of the avenacinase, Sap1, protein of *I. mors-panacis* (IMP), *I. robusta* (IR), and *I. europaea* isolates (Table 1). The avenacinase proteins were identified based on BLASTP of the total predicted proteins of each genome using the Sap1 homology protein sequence of *Botrytis cinerea* (CAB61489.1) as a query. The cladogram was created using RAxML and viewed by MEGA6. Bootstrap values based on 1000 replicates are shown as a percent. The scale bar is based on the difference in aa sequences per site. Clusters marked as 1, 2, 3, and 4 refer to copies 1, 2, 3, and 4 of the predicted genes found in one or more of the genomes. Figure S9. Relatedness based on aa sequences of the mating type1-2-1 (MAT1-2-1) protein of *I. mors-panacis* (IMP), *I. robusta* (IR), and *I. europaea* isolates (Table 1). MAT1-2-1 proteins were identified based on BLASTP of the total predicted proteins of each genome using the mating-type 1-2-1 protein sequence of *F. graminearum* (AAG42810.1) as a query. The cladogram was created using RAxML and viewed by MEGA6. Bootstrap values based on 1000 replicates are shown as a percent. The scale bar is based on the difference in aa sequences

per site. Clusters marked as 1, 2, and 3 refer to copies 1, 2, and 3 of the predicted genes found in one or more of the genomes. Figure S10. Relatedness based on aa sequences of the mating type 1-1-3 (MAT1-1-3) proteins of *I. mors-panacis* (IMP), *I. robusta* (IR), and *I. europaea* isolates (Table 1). MAT1-1-3 proteins were identified based on BLASTP of the total predicted proteins of each genome using the mating-type 1-1-3 protein sequence of *F. graminearum* (AAG42812.1) as a query. The cladogram was created using RAxML and viewed by MEGA6. Bootstrap values based on 1000 replicates are shown as a percent. The scale bar is based on the difference in aa sequences per site. Clusters marked as 1 and 2 refer to copies 1 and 2 of the predicted genes found in one or more of the genomes.

Author Contributions: Conceptualization, P.H.G.; methodology, B.B., T.H., M.V. and P.H.G.; formal analysis, B.B., T.H., M.V. and P.H.G.; investigation, B.B., T.H., M.V. and P.H.G.; resources, P.H.G.; data curation, M.V.; writing—B.B.; writing—review and editing, B.B., T.H., M.V. and P.H.G.; visualization, B.B., T.H., M.V. and P.H.G.; supervision, P.H.G.; project administration, P.H.G.; funding acquisition, P.H.G. All authors have read and agreed to the published version of the manuscript.

Funding: This research was funded by the Ontario Ministry of Agriculture, Food, and Rural Affairs, grant number UofG2014-2041.

Data Availability Statement: All data, tables, and figures in this manuscript are original. The genomes of the *I. mors-panacis* and *I. robusta* isolates in this study are available through NCBI under BioProject PRJNA885578.

Acknowledgments: We wish to thank the Ontario Ginseng Growers Association for their assistance.

Conflicts of Interest: The authors declare no conflict of interest. The funders had no role in the design of the study; in the collection, analysis, or interpretation of data; in the writing of the manuscript; or in the decision to publish the results.

References

1. Sewell, G.F.W. Effects of *Pythium* species on the growth of apple and their possible causal role in apple replant disease. *Ann. App. Biol.* **1981**, *97*, 31–42. [CrossRef]
2. Petit, E.; Gubler, W.D. Characterization of *Cylindrocarpon* species, the cause of black foot disease of grapevine in California. *Plant Dis.* **2005**, *89*, 1051–1059. [CrossRef]
3. Seifert, K.A.; Axelrood, P.E. *Cylindrocarpon destructans* var. destructans. *Can. J. Plant Pathol.* **1998**, *20*, 115–117. [CrossRef]
4. Cabral, A.; Groenewald, J.Z.; Rego, C.; Oliveira, H.; Crous, P.W. *Cylindrocarpon* root rot: Multi-gene analysis reveals novel species within the *Ilyonectria radicicola* species complex. *Mycol. Prog.* **2012**, *11*, 655–688. [CrossRef]
5. Matuo, T.; Miyazawa, Y. On *Cylindrocarpon panacis* sp. nov. causing root rot of ginseng. *Trans. Mycol. Soc. Jpn.* **1969**, *9*, 109–112.
6. Reeleder, R.D.; Brammall, R.A. Pathogenicity of *Pythium* species, *Cylindrocarpon destructans*, and *Rhizoctonia solani* to ginseng seedlings in Ontario. *Can. J. Plant Pathol.* **1994**, *16*, 311–316. [CrossRef]
7. Matuo, T.; Miyazawa, Y. Scientific name of *Cylindrocarpon* sp. causing root rot of ginseng. *Ann. Phytopathol. Soc. Jpn.* **1984**, *50*, 649–652. [CrossRef]
8. Song, J.Y.; Seo, M.W.; Kim, S.I.; Nam, M.H.; Lim, H.S.; Kim, H.G. Genetic diversity and pathogenicity of *Cylindrocarpon destructans* isolates obtained from Korean *Panax ginseng*. *Mycobiology* **2014**, *42*, 174–180. [CrossRef]
9. Seo, M.W.; Park, J.Y.; Kim, S. Analysis of genetic diversity and PCR assay for the detection of ginseng root rot pathogen, *Ilyonectria radicicola*. *Res. Plant Dis.* **2015**, *21*, 121.
10. Reeleder, R.D.; Roy, R.; Capel, B. Seed and root rots of ginseng (*Panax quinquefolius* L.) caused by *Cylindrocarpon destructans* and *Fusarium* spp. *J. Ginseng Res.* **2002**, *26*, 151–158.
11. Li, T.S.C. Asian and American ginseng—A review. *HortTechnology* **1995**, *5*, 27–34. [CrossRef]
12. Rahman, M.; Punja, Z.K. Factors influencing development of root rot on ginseng caused by *Cylindrocarpon destructans*. *Phytopathology* **2005**, *95*, 1381–1390. [CrossRef]
13. Kernaghan, G.; Reeleder, R.D.; Hoke, S.M.T. Quantification of *Cylindrocarpon destructans* f. sp. *panacis* in soils by real-time PCR. *Plant Pathol.* **2007**, *56*, 508–516. [CrossRef]
14. Farh, M.E.; Kim, Y.J.; Kim, Y.J.; Yang, D.C. *Cylindrocarpon destructans*/*Ilyonectria radicicola*-species complex: Causative agent of ginseng root-rot disease and rusty symptoms. *J. Ginseng Res.* **2018**, *42*, 9–15. [CrossRef]
15. Westerveld, S.M.; Shi, F. The history, etiology, and management of ginseng replant disease: A Canadian perspective in review. *Can. J. Plant Sci.* **2021**, *101*, 886–901. [CrossRef]
16. Rafiqi, M.; Ellis, J.G.; Ludowici, V.A.; Hardham, A.R.; Dodds, P.N. Challenges and progress towards understanding the role of effectors in plant–fungal interactions. *Curr. Opin. Plant Biol.* **2012**, *15*, 477–482. [CrossRef]
17. Plissonneau, C.; Benevenuto, J.; Mohd-Assaad, N.; Fouché, S.; Hartmann, F.E.; Croll, D. Using population and comparative genomics to understand the genetic basis of effector-driven fungal pathogen evolution. *Front. Plant Sci.* **2017**, *8*, 119. [CrossRef]

18. Grunwald, B.; Vandooren, J.; Gerg, M.; Ahomaa, K.; Hunger, A.; Berchtold, S.; Akbareian, S.; Schaten, S.; Knolle, P.; Edwards, D.R.; et al. Systemic ablation of MMP-9 triggers invasive growth and metastasis of pancreatic cancer via deregulation of IL6 expression in the bone marrow. *Mol. Cancer Res.* **2016**, *14*, 1147–1158. [CrossRef]
19. Zeng, Z.; Sun, H.; Vainio, E.J.; Raffaello, T.; Kovalchuk, A.; Morin, E.; Duplessis, S.; Asiegbu, F.O. Intraspecific comparative genomics of isolates of the Norway spruce pathogen (*Heterobasidion parviporum*) and identification of its potential virulence factors. *BMC Genom.* **2018**, *19*, 220. [CrossRef]
20. Menardo, F.; Praz, C.R.; Wicker, T.; Keller, B. Rapid turnover of effectors in grass powdery mildew (*Blumeria graminis*). *BMC Evol. Biol.* **2017**, *17*, 223. [CrossRef]
21. Guan, Y.; Chen, M.; Ma, Y.; Du, Z.; Tuan, N.; Li, Y.; Xiao, J.; Zhang, Y. Whole-genome and time-course dual RNA-Seq analyses reveal chronic pathogenicity-related gene dynamics in the ginseng rusty root rot pathogen *Ilyonectria robusta*. *Sci. Rep.* **2020**, *10*, 1586. [CrossRef] [PubMed]
22. Zhu, B.; Wang, S.; Mi, C.Y.; Yang, R.H.; Zen, G.H.; Hu, X.F. Genome sequence resource for *Ilyonectria mors-panacis*, causing rusty root rot of *Panax notoginseng*. *Mol. Plant-Microbe Interact.* **2019**, *32*, 1468–1471. [CrossRef] [PubMed]
23. Edwards, K.; Johnstone, C.; Thompson, C. A simple and rapid method for the preparation of plant genomic DNA for PCR analysis. *Nucleic Acids Res.* **1991**, *19*, 1349. [CrossRef] [PubMed]
24. Camacho, C.; Coulouris, G.; Avagyan, V.; Ma, N.; Papadopoulos, J.; Bealer, K. BLAST plus: Architecture and applications. *BMC Bioinform.* **2009**, *10*, 421. [CrossRef]
25. Simão, F.A.; Waterhouse, R.M.; Ioannidis, P.; Kriventseva, E.V.; Zdobnov, E.M. BUSCO: Assessing genome assembly and annotation completeness with single-copy orthologs. *Bioinformatics* **2015**, *31*, 3210–3212. [CrossRef]
26. Stamatakis, A. RAxML version 8: A tool for phylogenetic analysis and post-analysis of large phylogenies. *Bioinformatics* **2014**, *30*, 1312–1313. [CrossRef]
27. Paradis, E.; Schliep, K. ape 5.0: An environment for modern phylogenetics and evolutionary analyses in R. *Bioinformatics* **2018**, *35*, 526–528. [CrossRef]
28. Taylor, A.; Vagany, A.; Jackson, A.C.; Harrison, R.J.; Rainoni, A.; Clarkson, J.P. Identification of pathogenicity-related genes in *Fusarium oxysporum* f. sp. *cepae*. *Mol. Plant Pathol.* **2016**, *17*, 1032–1047. [CrossRef]
29. Lievens, B.; Houterman, P.M.; Rep, M. Effector gene screening allows unambiguous identification of *Fusarium oxysporum* f. sp. lycopersici races and discrimination from other formae specialis. *FEMS Microbiol. Lett.* **2009**, *300*, 201–215. [CrossRef]
30. Hissen, A.H.; Wan, A.N.; Warwas, M.L.; Pinto, L.J.; Moore, M.M. The *Aspergillus fumigatus* siderophore biosynthetic gene sidA, encoding L-ornithine N5-oxygenase, is required for virulence. *Infect. Immun.* **2005**, *73*, 5493–5503. [CrossRef]
31. Wight, W.D.; Labuda, R.; Walton, J.D. Conservation of the genes for HC-toxin biosynthesis in *Alternaria jesenskae*. *BMC Microbiol.* **2013**, *13*, 165. [CrossRef]
32. Quidde, T.; Buttner, P.; Tudzynski, P. Evidence for three different specific saponin-detoxifying activities in *Botrytis cinerea* and cloning and functional analysis of a gene coding for a putative avenacinase. *Eur. J. Plant Pathol.* **1999**, *105*, 273–283. [CrossRef]
33. Yun, S.H.; Arie, T.; Kaneko, I.; Yoder, O.C.; Turgeon, G. Molecular organization of mating type loci in heterothallic, homothallic, and asexual *Gibberella/Fusarium* species. *Fungal Genet. Biol.* **2000**, *31*, 7–20. [CrossRef]
34. Farh, M.E.; Han, J.A.; Kim, Y.J.; Kim, J.C.; Singh, P.; Yang, D.C. Discovery of a new primer set for detection and quantification of *Ilyonectria mors-panacis* in soils for ginseng cultivation. *J. Ginseng Res.* **2019**, *43*, 1–9. [CrossRef]
35. Seifert, K.A.; McMullen, C.R.; Yee, D.; Reeleder, R.D.; Dobinson, K.F. Molecular differentiation and detection of ginseng adapted isolates of the root rot fungus *C. destructans*. *Popul. Biol.* **2003**, *93*, 1533–1542. [CrossRef]
36. Raffaele, S.; Kamoun, S. Genome evolution in filamentous plant pathogens: Why bigger can be better. *Nat. Rev. Microbiol.* **2012**, *10*, 417–430. [CrossRef]
37. Spanu, P.D.; Abbott, J.C.; Amselem, J.; Burgis, T.A.; Soanes, D.M.; Stüber, K.; Van Themaat, E.V.L.; Brown, J.K.M.; Butcher, S.A.; Gurr, S.I.; et al. Genome expansion and gene loss in powdery mildew fungi reveal tradeoffs in extreme parasitism. *Science* **2010**, *330*, 1543–1546. [CrossRef]
38. Noble, L.M.; Andrianopoulos, A. Fungal genes in context: Genome architecture reflects regulatory complexity and function. *Genome Biol. Evol.* **2013**, *5*, 1336–1352. [CrossRef]
39. Vogelgsang, S.; Widmer, F.; Jenny, E.; Enkerl, J. Characterisation of novel *Fusarium graminearum* microsatellite markers in different *Fusarium* species from various countries. *Eur. J. Plant Pathol.* **2008**, *123*, 477–482. [CrossRef]
40. Van der burgt, A.; Karimi Jashni, M.; Bahkali, A.H.; De Wit, P.J.G.M. Pseudogenization in pathogenic fungi with different host plants and lifestyles might reflect their evolutionary past. *Mol. Plant Pathol.* **2014**, *15*, 133–144. [CrossRef]
41. Lafontaine, I.; Dujon, B. Origin and fate of pseudogenes in Hemiascomycetes: A comparative analysis. *BMC Genom.* **2010**, *11*, 260. [CrossRef] [PubMed]
42. Lim, S.; Notley-McRobb, L.; Lim, M.; Carter, D.A. A comparison of the nature and abundance of microsatellites in 14 fungal genomes. *Fungal Genet. Biol.* **2004**, *41*, 1025–1036. [CrossRef] [PubMed]
43. Testa, A.C.; Oliver, R.P.; James, K.; Hane, J.K. OcculterCut: A comprehensive survey of AT-rich regions in fungal genomes. *Genome Biol. Evol.* **2016**, *8*, 2044–2064. [CrossRef] [PubMed]
44. Haas, H.; Eisendle, M.; Turgeon, B.G. Siderophores in fungal physiology and virulence. *Annu. Rev. Phytopathol.* **2008**, *46*, 149–187. [CrossRef]

45. Walsh, J.; DesRochers, N.; Renaud, J.B.; Seifert, K.A.; Yeung, K.K.C.; Sumarah, M.W. Identification of N,N′,N″-triacetylfusarinine C as a key metabolite for root rot disease virulence in American ginseng. *J. Ginseng Res.* **2019**, *45*, 156–162. [CrossRef]
46. Brosch, G.; Ransom, R.; Lechner, T.; Walton, J.D.; Loidl, P. Inhibition of maize histone deacetylases by HC toxin, the host-selective toxin of *Cochliobolus carbonum*. *Plant Cell* **1995**, *7*, 1941–1950.
47. Bernards, M.A.; Ivanov, D.A.; Neculai, M.A.; Nicol, R.W. Ginsenosides: Phytoanticipins or host recognition factors? In *The Biological Activity of Phytochemicals*; Gang, D.R., Ed.; Springer: New York, NY, USA, 2011; pp. 13–46.
48. Searels, J.M.; Keen, K.D.; Horton, J.L.; Clarke, H.D.; Ward, J.R. Comparing ginsenoside production in leaves and roots of wild American ginseng (*Panax quinquefolius*). *Am. J. Plant Sci.* **2013**, *4*, 1252–1259. [CrossRef]
49. Farh, M.E.; Kim, Y.J.; Abbai, R.; Singh, P.; Jung, K.H.; Kim, Y.J.; Yang, D.C. Pathogenesis strategies and regulation of ginsenosides by two species of *Ilyonectria* in *Panax ginseng*: Power of speciation. *J. Ginseng Res.* **2020**, *44*, 332–340. [CrossRef]
50. Klix, V.; Nowrousian, M.; Ringelberg, C.; Loros, J.J.; Dunlap, J.C.; Pöggeler, S. Functional characterization of MAT1-1-specific mating-type genes in the homothallic ascomycete *Sordaria macrospora* provides new insights into essential and nonessential sexual regulators. *Eukaryot. Cell* **2010**, *9*, 894–905. [CrossRef]
51. Martin, S.H.; Wingfield, B.D.; Wingfield, M.J.; Steenkamp, E.T. Causes and consequences of variability in peptide mating pheromones of Ascomycete fungi. *Mol. Biol. Evol.* **2011**, *28*, 1987–2003. [CrossRef]
52. Turgeon, G.; Yoder, O.C. Proposed nomenclature for mating type genes of filamentous Ascomycetes. *Fungal Genet. Biol.* **2000**, *31*, 1–5. [CrossRef]
53. Degnan, J.H.; Rosenberg, N.A. Gene tree discordance, phylogenetic inference and the multispecies coalescent. *Trends Ecol. Evol.* **2009**, *24*, 332–340. [CrossRef]
54. Jashni, M.K.; Dols, I.H.; Iida, Y.; Boeren, S.; Beenen, H.G.; Mehrabi, R.; Collemare, J.; de Wit, P.J.G.M. Synergistic action of a metalloprotease and a serine protease from *Fusarium oxysporum* f. sp. *lycopersici* cleaves chitin-binding tomato chitinases, reduces their antifungal activity, and enhances fungal virulence. *Mol. Plant-Microbe Interact.* **2015**, *28*, 996–1008. [CrossRef]